Hindawi Publishing Corporation
Journal of Nanomaterials
Volume 2011, Article ID 534647, 7 pages
doi:10.1155/2011/534647

Research Article

Structural and Mechanical Properties of CrN_x Coatings Deposited by Medium-Frequency Magnetron Sputtering with and without Ion Source Assistance

Can Xin Tian,[1] Bing Yang,[2] Jun He,[1] Hong Jun Wang,[1] and De Jun Fu[1]

[1] *Department of Physics and Key Laboratory of Artificial Micro- and Nano-Materials of Ministry of Education, Wuhan University, 430072 Wuhan, China*
[2] *School of Power and Mechanical Engineering, Wuhan University, 430072 Wuhan, China*

Correspondence should be addressed to De Jun Fu, djfu@whu.edu.cn

Received 4 May 2010; Revised 27 June 2010; Accepted 2 August 2010

Academic Editor: Bo Zou

CrN_x coatings were deposited on Si (100) and WC-Co substrates by a home-made medium-frequency magnetron sputtering system with and without thermal filament ion source assistance. The structure and composition of the coatings were characterized by X-ray diffraction, atomic force microscopy, scanning electron microscopy, and transmission electron microscopy. The mechanical and tribological properties were assessed by microhardness and pin-on-disc testing. The ion source-assisted system showed a deposition rate of 3.88 μm/h, much higher than the value 2.2 μm/h without ion source assistance. The CrN_x coatings prepared with ion source assistance exhibited an increase in microhardness (up to 16.3 GPa) and adecrease in friction coefficient (down to 0.48) at the optimized cathode source-to-substrate distance.

1. Introduction

Transition metal nitrides, especially chromium nitride (CrN), have been studied extensively due to their unique properties, including high hardness, good wear resistance, as well as excellent corrosion and high-temperature oxidation resistance [1–4]. They are widely applied in industry as protective coatings [5–7]. Recent studies also revealed magnetic properties in CrN, and it might find applications in the electronic industries [8, 9]. Many methods have been used for the deposition of CrN films, among which unbalanced magnetron sputtering produces good quality samples at high-deposition rates [2]. The pulsed DC reactive magnetron sputtering technique was characterized by improved ionization and a high ion-to-neutral particle ratio during deposition to enhance the quality of coatings [10], but more importantly it increased the kinetic energy of the ions in the plasma, which can enhance the ion bombardment of the substrate and film [11–14]. Therefore, high-quality CrN coatings have been prepared by pulsed dc magnetron sputtering [15, 16], and the high-power pulsed magnetron sputtering has also been developed for deposition of CrN coatings [17, 18]. It is known that low ionization efficiency in the plasma is a hurdle of magnetron sputtering; therefore, plasma or ion sources have been developed to improve ionization efficiency [19, 20]. In particular, Wei et al. reported dense and thick films of transition metal nitrides, including ZrN and TiN, by means of plasma-enhanced magnetron sputtering, where an electron source of thermal filament type is a key technology [21, 22]. In order to prepare thick protective coatings with high deposition rate, high microhardness, and ideal surface chemistry, it is necessary to introduce high-density plasma in pulsed dc magnetron sputtering systems.

In this paper, we have prepared CrN_x coatings at various magnetron cathode source-substrate distances by medium-frequency (40 kHz) magnetron sputtering with a thermal filament ion source and conducted characterization in comparison with samples prepared without the use of the ion source. We intended to find out the influence of cathode source-to-substrate distances and ion source on the deposition rate, microstructural, mechanical, and

tribological properties. Then, we have optimized the source-substrate distance at which the ion source best assists the deposition process, producing CrN_x coatings with superior properties.

2. Experiment Details

The CrN_x coatings were deposited by using a modified closed field twin unbalanced magnetron sputtering system. The vacuum chamber is $\phi 400 \times 500$ mm in dimension. The ion source was powered by a supply of 20 A and 24 V and was mounted in the middle-upper area of the chamber. Cr sheets with a purity of 99.99% and an area of $10 \times 40\,cm^2$ were used as a cathode source material. Prior to deposition, a base pressure was less than 5×10^{-3} Pa. For substrates, p-type Si (100) and mirror-polished WC-Co plates were ultrasonically cleaned in acetone and methanol, rinsed in de-ionized water, and dried in N_2 before being loaded into the deposition chamber. Then, they were ion etched for 30 min in Ar atmosphere at a pressure of 2.0 Pa and a negative bias voltage of 800 V applied to the substrate holder. N_2 (99.99%) and Ar (99.99%) were used as working gases. First, a layer of pure Cr (about 230 nm) was deposited onto the substrate for 5 min in Ar ambient at 0.25 Pa and −100 V to improve the adhesion. Then, N_2 was let in, and Ar flow rate was tuned to keep an $Ar : N_2$ ratio of 1 : 1. The total pressure was kept at 0.25 Pa, and the substrate bias was fixed at −100 V. The medium-frequency power used was 7.0 kW, and cathode source-substrate distance was varied between 50 and 140 mm. The substrates temperature was kept at 150°C. The ion source was a tungsten filament which emitted electrons when heated by a high current and could produce ions of argon gas fed to the outlet of the filament source. The ion source was installed at the upper part of the chamber, similar to the configuration described in the literature [23].

The crystal structure of the deposited CrN_x coatings was characterized by X-ray diffraction (XRD, Bruker-Axs D8 advanced which was operated at voltage and current of 40 kV and 40 mA, resp.) with a Cu ka radiation and JEOL JEM 2010 transmission electron microscopy (TEM). The deposition rate was evaluated from the thickness of the films measured with a FTSS2-S4L-3D step profiler. The cross-section micrographs were measured using Sirion FEG scanning electron microscopy (SEM), and the composition of CrN_x coatings was determined by using an EDAX genesis 7000 energy dispersive spectroscopy (EDS) system operated at 12 kV. The surface topography was analyzed using an atomic force microscope (AFM) (Shimadzu SPM-9500J3) operated in the tapping mode. The hardness was measured using an HX-1000 microhardness tester with a load of 25 g (the indentation depth was about 250 nm) and taking the average of 5 values. The friction and wear measurements of the CrN_x coatings were carried out by using an MS-T3000 ball-on-disk tester which slides in ambient air at 30°C, at relative humidity of 70%, with a Si_3N_4 ball of 3 mm in diameter being used as the mating material, on which a 4 N load was applied. The average sliding speed was 0.02 m/s for a fixed sliding time of 30 min, and the friction coefficients were recorded during the test.

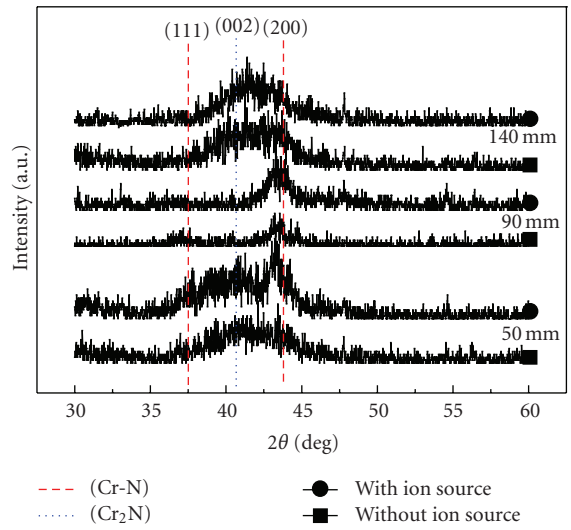

Figure 1: XRD patterns of CrN_x coatings deposited at various d_{ss}.

3. Results and Discussion

Figure 1 shows the XRD spectra of CrN_x coatings deposited under various source-substrate distances, d_{ss}. The CrN_x coatings contain two phases of fcc CrN and hexangular Cr_2N, their corresponding PDF numbers being 65-2899 and 79-2159, respectively. Only the CrN (200) peak is observed for the coating deposited at $d_{ss} = 90$ mm. With increasing d_{ss}, the XRD data show the structure of the CrN_x coatings to be changed from CrN to a mixture of Cr_2N + CrN. At the lower extreme, $d_{ss} = 50$ mm, the planes of Cr_2N (002), together with CrN (200) and (111), can be seen whereas at larger distance of 140 mm, the films deposited exhibit inconspicuous overlap of Cr_2N (002) and CrN (200) orientations.

The energies of the depositing particles were different at different d_{ss} because of the collision of ions (N, Ar, and Cr). The particles bombarded the substrate and heat the substrate. The ratio of ion to neutral particles (Ar, N, and Cr) arriving at the growing film would be different at different d_{ss}. These factors influence the film growth kinetics, which finally determine the orientation and phase structure of the CrN_x coatings. The broadening of the diffraction peaks of CrN_x coatings is related to the changes in the grain size, thickness, and residual stress in the coating. The different ratio of N/Ar has an influence on the composition of CrN or Cr_2N [24]. Therefore, the formation of CrN or Cr_2N at different d_{ss} is attributed to the different N/Ar ratio influenced by d_{ss}.

Also shown in Figure 1 is the influence of the hot filament ion source; CrN_x coatings deposited with ion source assistance have different diffraction peaks at all values of d_{ss}. In particular, at d_{ss} of 90 mm, the intensity of (200) peak is enhanced. The slightly higher intensity of the XRD peaks in the CrN coatings deposited with the ion source assistance can be related to the enhanced ion bombardment from the plasma, which may lead to a higher substrate temperature as well as a higher ion-to-neutral particle ratio.

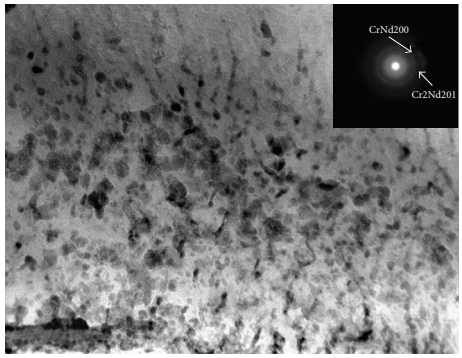

(a)

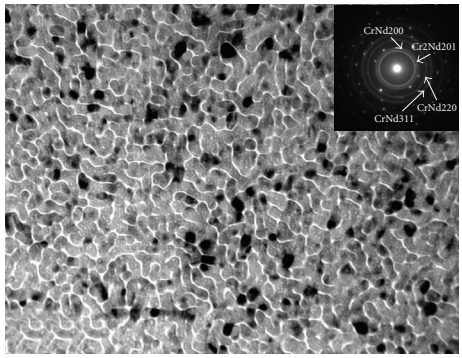

(b)

FIGURE 2: Bright-field TEM images and selected area diffraction of CrN_x coatings deposited at d_{ss} = 90 mm. The view directions are normal to the coating surface. (a) Samples prepared without ion source assistance, (b) with ion source assistance.

Figure 2(a) shows bright-field TEM images of CrN_x coatings deposited without ion source assistance, which reveals nonuniform CrN_x grains. The corresponding selected area diffraction pattern reveals obvious CrN and blurry Cr_2N phases. On the contrary, with the use of ion source Figure 2(b), uniform CrN_x grains are observed and selected area diffraction shows obvious diffraction rings of CrN and Cr_2N, revealing the polycrystalline nature of the film, with diffraction points attributed to the Si (100) substrate. The uniform CrN_x grains with distinct grain boundaries suggest higher microhardness of the corresponding coatings.

Figure 3 shows the deposition rate of the CrN_x coatings as a function of d_{ss}. As a general tendency, the deposition rate of the coatings decreases with increasing d_{ss}. The deposition rate is further increased at d_{ss} values of 90 mm and 140 mm with the assistance of the ion source. At d_{ss} = 50 mm, however, the ion source assistance tends to decrease the deposition rate.

At larger source-substrate spacing, the sputter-produced particles arriving at the substrate decrease in number due to the collision of Cr and N atoms with the plasma of N_2, Ar, N^+, Ar^+, and secondary electrons. However, with the use of thermal filament ion source, more ions, especially Ar ions, were generated, which bombarded the Cr target and produced more Cr particles [3, 25]. As a result, the deposition rate is higher than that without ion source assistance. At close source-substrate spacing (d_{ss} = 50 mm), with thermal filament ion source assistance, the increased amount of Ar and other ions causes severe re sputtering of the film surface. Therefore, the deposition rate becomes lower than that without ion source assistance. With the increase of d_{ss}, the energies of deposition particles decreased because of the collision in the plasma, especially at d_{ss} much larger than molecular mean-free-path. Hence, the deposition rate at larger d_{ss} with the ion source assistance becomes larger than without ion source assistance.

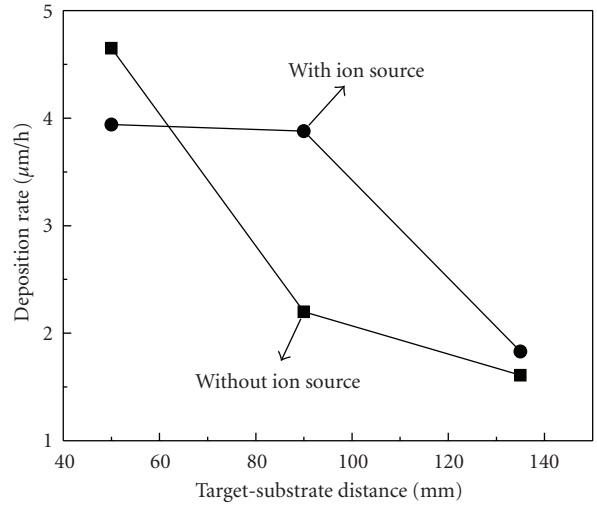

FIGURE 3: Deposition rate as a function of the d_{ss} of the CrN_x coatings.

Figure 4 shows typical three-dimensional AFM morphologies taken from the CrN_x coatings deposited at d_{ss} of 50, 90, and 140 mm without and with thermal filament ion source assistance. The topographies shown in Figure 4(a) suggest that the CrN_x coatings deposited at 50 mm are composed of columns with irregular tops. When the source-substrate spacing increases to 90 mm, the size of the extrusive tops was significantly reduced (Figure 4(b)). At even larger d_{ss}, the extrusive tops become more regular and an even smoother surface is observed (Figure 4(c)). Figure 5 shows the root-mean-square (RMS) roughness calculated from the AFM images of the CrN_x coatings deposited at various d_{ss} without and with thermal filament ion source assistance. Corresponding to the AFM observations in Figure 4, the RMS roughness of the CrN_x coatings deposited at 50 mm was relatively large at shorter source-substrate distance. The use of thermal filament ion source gives rise to the reduction of RMS roughness from 10.3 to 8.6 nm at d_{ss} = 50 mm. At larger source-substrate distance, the difference becomes negligible.

When the source-substrate spacing is small, the deposition rate is high (Figure 3) and the growth is columnar, which gives a large roughness. More energetic ions bombard the substrate, which affected the nucleation kinetics [26], resulting in rapid growth of the grain, thereby exhibiting larger

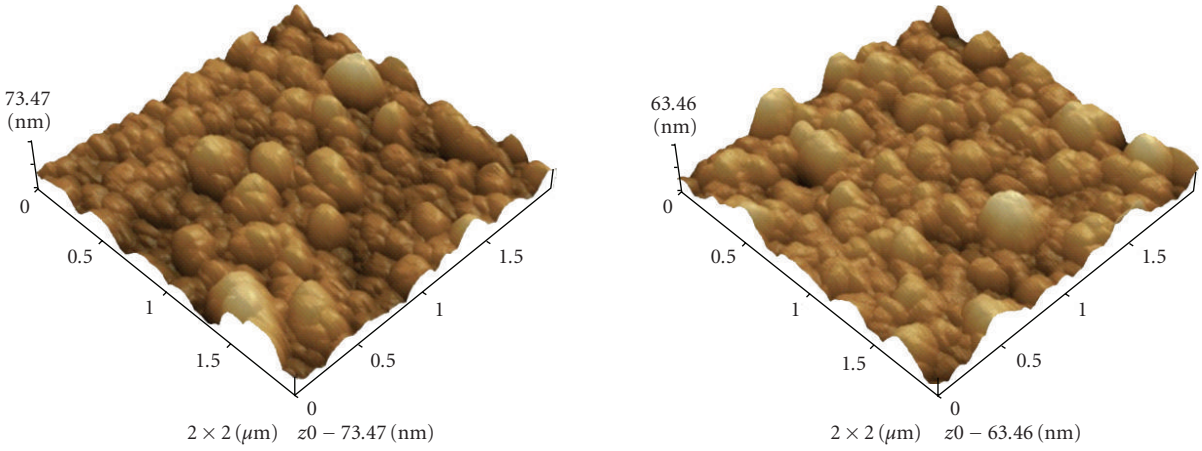

(a)

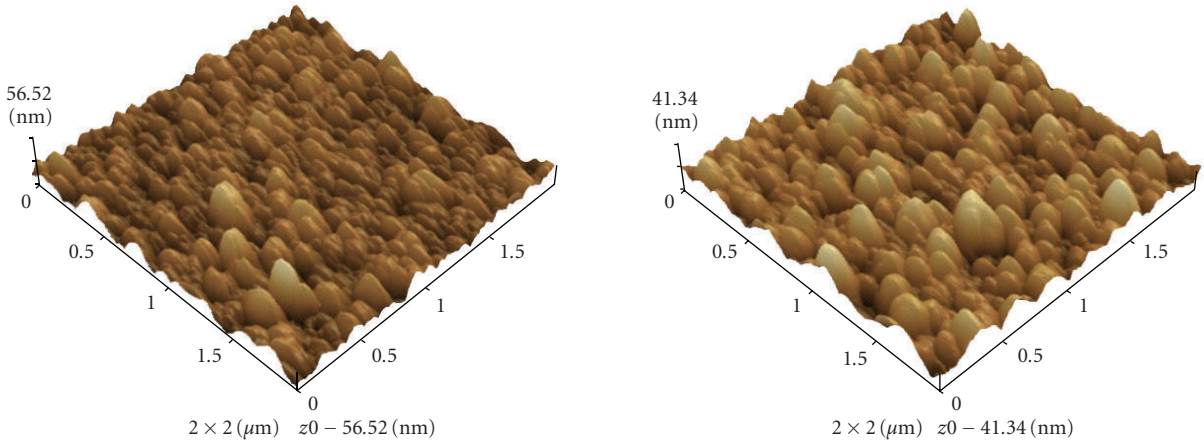

(b)

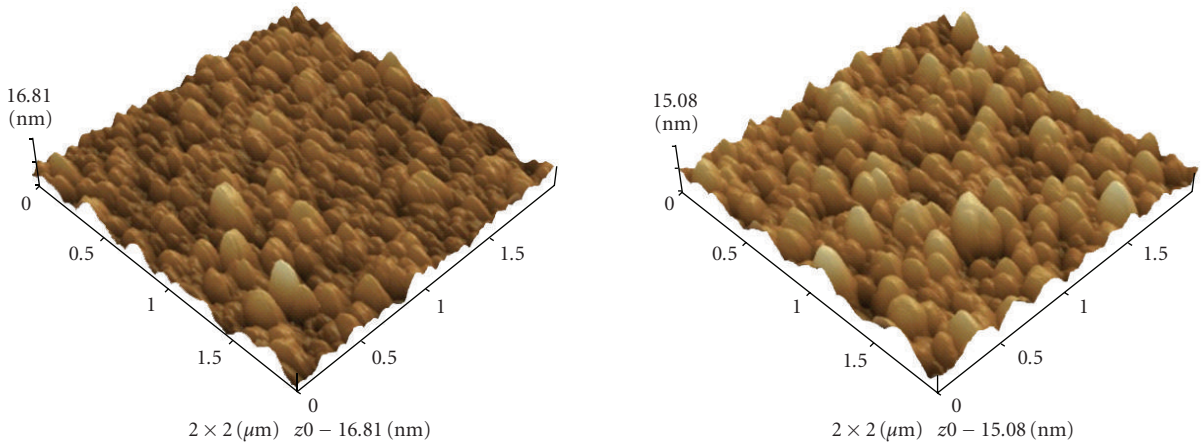

(c)

FIGURE 4: AFM morphologies of CrN_x coatings deposited at d_{ss} of 50 mm (a), 90 mm (b), and 140 mm (c). The images on the left-hand side are of samples prepared without ion source, and those on the right-hand side are of samples prepared with ion source assistance.

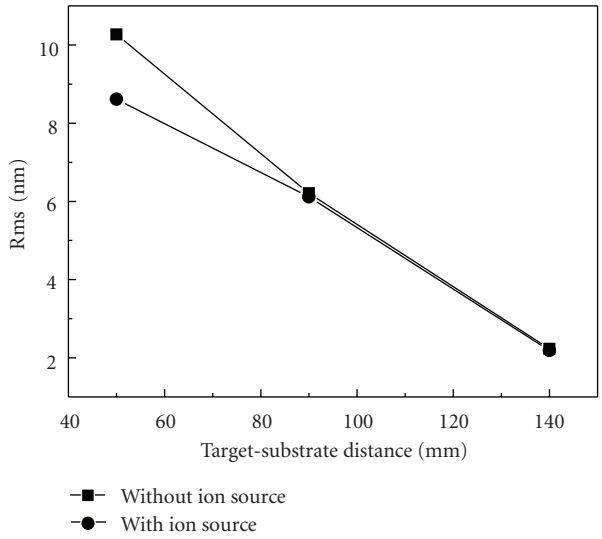

Figure 5: Variation in rms roughness measured from AFM images of the CrN_x coatings as a function of d_{ss}.

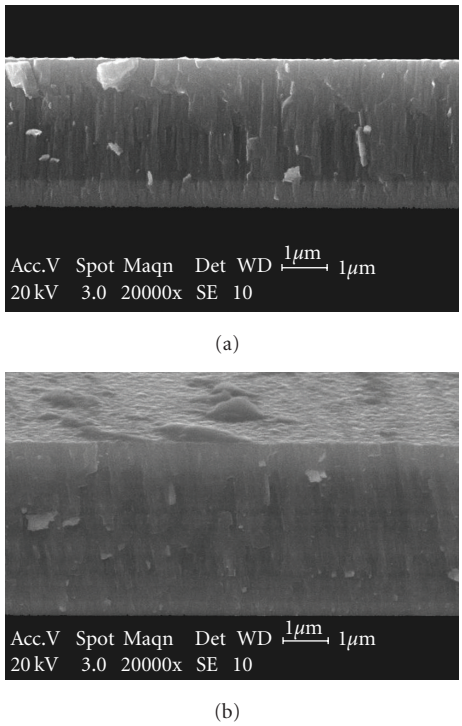

Figure 6: Cross-sectional SEM image of CrN_x coatings deposited at d_{ss} = 90 mm (a) without and (b) with ion source assistance.

particle sizes. With increasing d_{ss}, frequent collision reduces the kinetic energies of particles reaching the surface, and the deposition is slowed down, leading to uniform surfaces with extrusions of smaller particle size and higher density.

Figure 6 shows cross-section SEM images of the CrN_x coatings deposited without and with ion source assistance at

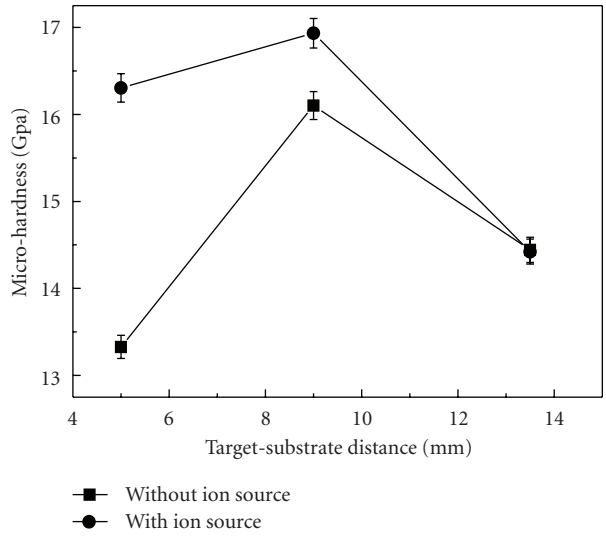

Figure 7: Variation of microhardness of CrN_x coatings as a function of d_{ss}.

d_{ss} of 90 mm. One sees a columnar growth throughout the whole film thickness without the ion source assistance. In the process of using ion source, columnar growth is not obvious and the coating becomes denser, apparently resulting from the energetic bombardment by ions produced with the ion source assistance.

Figure 7 shows the microhardness of the CrN_x coatings as a function of source-substrate distance, which exhibits the same trend, but the values are higher when ion source assistance is applied during deposition. At d_{ss} = 90 mm, the highest hardness is observed. This is accounted for by better crystallization and higher N concentration (measured by EDS) measured from the samples. The CrN_x coating deposited with the thermal filament ion source had higher N concentration (as shown in Figure 8), and the films were denser, with much finer grains (as shown Figure 2). It is believed that the grain size rather than the existence of Cr_2N phase influences the hardness values [27], which explains the further improvement of the microhardness at d_{ss} = 90 mm.

Figure 9 shows the friction coefficients of CrN_x coatings. The average friction coefficient of the CrN_x films prepared without ion source is 0.53 and is decreased to 0.48 with ion source assistance. This is consistent with the enhanced microhardness and the reduction in the surface roughness of the CrN_x coatings.

4. Conclusion

We have prepared CrN_x coatings by medium-frequency magnetron sputtering and demonstrated the improvement of the structural and mechanical properties of coatings by introducing thermal filament ion source during deposition. The CrN_x coatings deposited with ion source assistance exhibited an increase in microhardness from 13.25–16.3 GPa at a source-substrate distance of 50 mm and from

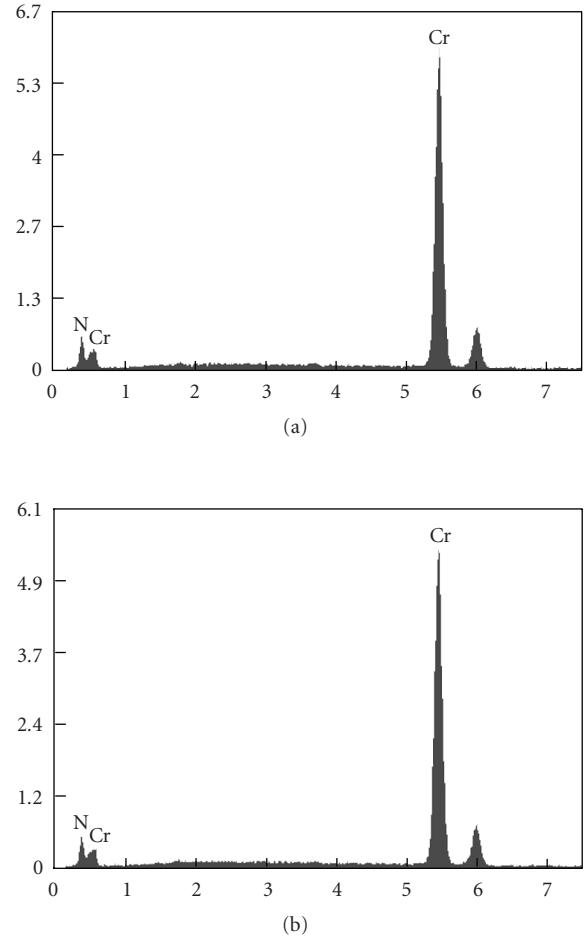

Figure 8: The EDS images of CrNx coatings deposited at Dts = 90 mm. (a) Samples without ion source assistance, N/Cr = 0.9075; (b) with ion source assistance, N/Cr = 0.9242.

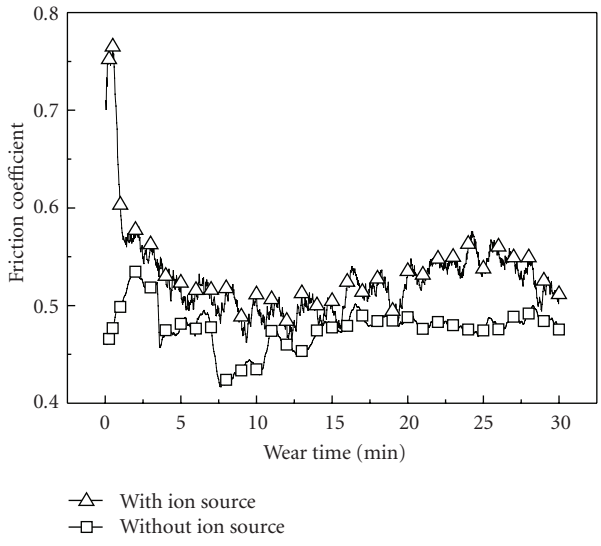

Figure 9: Variation of friction coefficient with sliding time of CrN_x coatings at d_{ss} = 90 mm.

16.0-17.0 GPa at the optimized d_{ss} of 90 mm. The friction coefficient was decreased typically from 0.53–0.48. A deposition rate of 3.88 μm/h was achieved, and the roughness was 6.0 nm for the coatings deposited at d_{ss} of 90 mm. The results show that the use of simple ion source assistance may be promising for high-rate deposition of CrN_x coatings.

Acknowledgment

This paper was supported by the NSFC under Contract 50905130, China Ministry of Industry and Information Technology under 2009ZX04012-032, Doctoral Fund of Ministry of Education of China for the New Teacher (20090141120067), and the Fundamental Research Funds for the Central Universities.

References

[1] X. M. He, N. Baker, B. A. Kehler, K. C. Walter, M. Nastasi, and Y. Nakamura, "Structure, hardness, and tribological properties of reactive magnetron sputtered chromium nitride films," *Journal Vacuum Science Technology A*, vol. 18, no. 1, pp. 30–36, 2000.

[2] J. J. Olaya, S. E. Rodil, S. Muhl, and E. Sánchez, "Comparative study of chromium nitride coatings deposited by unbalanced and balanced magnetron sputtering," *Thin Solid Films*, vol. 474, no. 1-2, pp. 119–126, 2005.

[3] G. A. Zhang, P. X. Yan, P. Wang, Y. M. Chen, and J. Y. Zhang, "Influence of nitrogen content on the structural, electrical and mechanical properties of CrNx thin films," *Materials Science and Engineering A*, vol. 460-461, pp. 301–305, 2007.

[4] P. H. Mayrhofer, H. Willmann, and C. Mitterer, "Oxidation kinetics of sputtered Cr-N hard coatings," *Surface and Coatings Technology*, vol. 146-147, pp. 222–228, 2001.

[5] B. Warcholiński, A. Gilewicz, Z. Kukliński, and P. Myśliński, "Arc-evaporated CrN, CrN and CrCN coatings," *Vacuum*, vol. 83, no. 4, pp. 715–718, 2008.

[6] C. Öner, H. Hazar, and M. Nursoy, "Surface properties of CrN coated engine cylinders," *Materials and Design*, vol. 30, no. 3, pp. 914–920, 2009.

[7] S. H. Shin, M. W. Kim, M. C. Kang, K. H. Kim, D. H. Kwon, and J. S. Kim, "Cutting performance of CrN and Cr-Si-N coated end-mill deposited by hybrid coating system for ultra-high speed micro machining," *Surface and Coatings Technology*, vol. 202, no. 22-23, pp. 5613–5616, 2008.

[8] A. Ney, R. Rajaram, S. S. P. Parkin, T. Kammermeier, and S. Dhar, "Magnetic properties of epitaxial CrN films," *Applied Physics Letters*, vol. 89, no. 11, Article ID 112504, 3 pages, 2006.

[9] W. J. Feng, D. Li, W. F. Li et al., "Structure and magnetic properties of Cr(N)-β-Cr_2N nanoparticles prepared by arc-discharge," *Journal of Alloys and Compounds*, vol. 425, no. 1-2, pp. 4–9, 2006.

[10] J.-W. Lee, S.-K. Tien, Y.-C. Kuo, and C.-M. Chen, "The mechanical properties evaluation of the CrN coatings deposited by the pulsed DC reactive magnetron sputtering," *Surface and Coatings Technology*, vol. 200, no. 10, pp. 3330–3335, 2006.

[11] J. Lin, Z. L. Wu, X. H. Zhang, B. Mishra, J. J. Moore, and W. D. Sproul, "A comparative study of CrNx coatings Synthesized by DC and pulsed DC magnetron sputtering," *Thin Solid Films*, vol. 517, no. 6, pp. 1887–1894, 2009.

[12] J. Lin, J. J. Moore, B. Mishra, M. Pinkas, W. D. Sproul, and J. A. Rees, "Effect of asynchronous pulsing parameters on the structure and properties of CrAlN films deposited by pulsed closed field unbalanced magnetron sputtering (P-CFUBMS)," *Surface and Coatings Technology*, vol. 202, no. 8, pp. 1418–1436, 2008.

[13] C. Muratore, J. J. Moore, and J. A. Rees, "Electrostatic quadrupole plasma mass spectrometer and Langluir probe measurements of mid-frequency pulsed DC magnetron discharges," *Surface and Coatings Technology*, vol. 163-164, pp. 12–18, 2003.

[14] J. W. Bradley, H. Bäcker, Y. Aranda-Gonzalvo, P. J. Kelly, and R. D. Arnell, "The distribution of ion energies at the substrate in an asymmetric bi-polar pulsed DC magnetron discharge," *Plasma Sources Science and Technology*, vol. 11, no. 2, pp. 165–174, 2002.

[15] T. Elangovan, P. Kuppusami, R. Thirumurugesan, V. Ganesan, E. Mohandas, and D. Mangalaraj, "Nanostructured CrN thin films prepared by reactive pulsed DC magnetron Sputtering," *Materials Science and Engineering B*, vol. 167, no. 1, article 17, 2010.

[16] J.-W. Lee, Y.-C. Kuo, C.-J. Wang, L.-C. Chang, and K.-T. Liu, "Effects of substrate bias frequencies on the characteristics of chromium nitride coatings deposited by pulsed DC reactive magnetron sputtering," *Surface and Coatings Technology*, vol. 203, no. 5–7, pp. 721–725, 2008.

[17] J. Lin, J. J. Moore, W. D. Sproul, B. Mishra, Z. Wu, and J. Wang, "The structure and properties of chromium nitride coatings deposited using DC, pulsed DC and modulated pulse power magnetron sputtering," *Surface and Coatings Technology*, vol. 204, no. 14, pp. 2230–2239, 2010.

[18] A. P. Ehiasarian, W.-D. Münz, L. Hultman, U. Helmersson, and I. Petrov, "High power pulsed magnetron sputtered CrNx films," *Surface and Coatings Technology*, vol. 163-164, pp. 267–272, 2003.

[19] X. Yu, C. Wang, Y. Liu, D. Yu, and T. Xing, "Recent developments in magnetron sputtering," *Plasma Science and Technology*, vol. 8, no. 3, pp. 337–343, 2006.

[20] G. Li, C. Liu, J. Li, C. Zhang, Z. Mu, and Z. Long, "Plasma-ion beam source enhanced deposition system," *Surface and Coatings Technology*, vol. 193, no. 1–3, pp. 112–116, 2005.

[21] R. Wei, J. J. Vajo, J. N. Matossian, and M. N. Gardos, "Aspects of plasma-enhanced magnetron-sputtered deposition of hard coatings on cutting tools," *Surface and Coatings Technology*, vol. 158-159, pp. 465–472, 2002.

[22] R. Wei, "Plasma enhanced magnetron sputter deposition of Ti-Si-C-N based nanocomposite coatings," *Surface and Coatings Technology*, vol. 203, no. 5–7, pp. 538–544, 2008.

[23] R. Wei, E. Lang, C. Rincon, and J. H. Arps, "Deposition of thick nitrides and carbonitrides for sand erosion protection," *Surface and Coatings Technology*, vol. 201, no. 7, pp. 4453–4459, 2006.

[24] M. L. Kuruppu, G. Negrea, I. P. Ivanov, and S. L. Rohde, "Monolithic and multilayer Cr/CrN, Cr/Cr_2N, and Cr_2N/CrN coatings on hard and soft substrates," *Journal of Vacuum Science and Technology A*, vol. 16, no. 3, pp. 1949–1955, 1998.

[25] Y. M. Lu, W. S. Hwang, W. Y. Liu, and J. S. Yang, "Effect of RF power on optical and electrical properties of ZnO thin film by magnetron sputtering," *Materials Chemistry and Physics*, vol. 72, no. 2, pp. 269–272, 2001.

[26] C.-L. Huang and Y.-B. Chen, "The effect of deposition temperature and RF power on the electrical and physical properties of the MgTiO3 thin films," *Journal of Crystal Growth*, vol. 285, no. 4, pp. 586–594, 2005.

[27] P. H. Mayrhofer, G. Tischler, and C. Mitterer, "Microstructure and mechanical/thermal properties of Cr-N coatings deposited by reactive unbalanced magnetron sputtering," *Surface and Coatings Technology*, vol. 142–144, pp. 78–84, 2001.